Effects of Curved-Beam Heights to Harvested Energy in a Blanaced Comb-Drive Configuration

Dooyoung Hah
Department of Electrical and Electronics Engineering
Abdullah Gül University
Kayseri, Turkey
dooyoung.hah@agu.edu.tr

2021 Symposium on Design, Test, Integration & Packaging of MEMS and MOEMS (DTIP) | 978-1-6654-0230-9/21/$31.00 ©2021 IEEE | DOI: 10.1109/DTIP54218.2021.9568673

***Abstract*—Energy harvesting devices have been gaining increasing interests, especially in the areas of internet of things (IoTs) and sensor networks. Due to the broadband and random nature of typical vibration energy sources available in the environment, significant amount of research efforts have been put into the bandwidth broadening of the energy harvesters. Utilization of spring nonlinearity has been one of the most studied subject in that regard. In this work, response of an energy harvesting device with curved-beam springs to colored-noise vibration is studied numerically, based on stochastic differential equations. The harvester considered in this study is an electrostatic type with electrets and a balanced comb-drive configuration. The study mainly focuses on the effect of the beam height to the harvested power. The results show that curved-beam springs can increase the harvested electric power by 52% (2.69 mW versus 1.77 mW) in comparison to straight-beam springs of the same dimensions. Buckling-induced rapid snapping of the curved beams is attributed to such a power increase.**

Keywords—Energy harvesters, electrets, curved-beam springs, stochastic differential equations

I. Introduction

Energy harvesting has become an important subject for various fields, most notably for internet of things (IoTs), wireless sensor networks (WSNs), and implantable medical devices (IMDs). Vibration is one of the major energy sources with its widespread availability. Among various research directions in relation to the vibration energy harvesters (VEHs), bandwidth broadening has been one of the crucial topics due to the broadband and dynamic nature of most of the environmental vibration sources. Different approaches have been attempted so far, such as Duffing oscillators [1-3], harvester arrays [4,5], and multi-degree-of-freedom structures [6-8]. Yet, another approach is to utilize spring nonlinearity, for example, by employing clamped-clamped curved-beam springs [9-14]. This last approach is particularly interesting at the MEMS scale with its compact structure.

For the energy transduction, electrostatic, piezoelectric, electromagnetic, and thermoelectric mechanisms have been utilized most frequently. Among them, electrostatic one is advantageous due to its CMOS process compatibility and high power density. More particularly, electrostatic energy harvesters that employ electrets are interesting, which leads to simple electric circuitry [15-18].

This paper presents colored-noise responses of electret-based energy harvesters. The main aim of the study is to understand the effect of beam height of the curved beams to the harvested power. Numerical simulation based on stochastic differential equations was used for the study.

II. Device Structure and Operation Principle

Fig. 1 illustrates the conceptual sketch of the device structure. A moving part is engaged with two comb-drives, and anchored to the substrate through curved-beam springs. The comb-drives form electrets, whose dielectrics can be charged via soft X-ray or polarization. When the moving part moves in response to external vibration, it leads to charge movement, generating electric power. A proof mass (m, not shown in Fig.1) is attached on the moving part in order to enhance the device response at low frequency (< 250 Hz).

The electrode structure as well as the device geometries (summarized in Table I) of the study follows loosely that of the balanced comb-drive device reported in [17]. One of the most important design parameters is the as-fabricated height of the beam (h), which determines the snapping behavior of the beam. Snapping increases the motion of the actuators, and hence the harvested electric power. In addition, the spring nonlinearity that is responsible for such a snapping broadens the power spectrum.

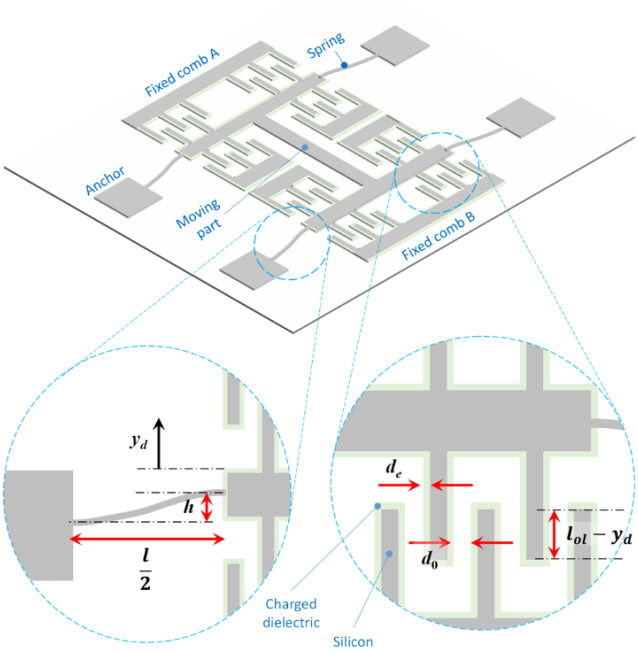

Fig. 1. Conceptual sketch of the energy harvester with electrets and curved-beam springs. Not to scale. A proof mass is not included in the sketch for clarity.

978-1-6654-0230-9/21/$31.00 ©2021 IEEE

TABLE I. DEVICE GEOMETRIES AND MATERIAL PROPERTIES

Description	*Symbol*	*Value*
Spring (length × width)	$l \times W$	8000 × 30 μm^2
Device layer thinkness	T	400 μm
Comb-drive number of fingers	N_f	900
Finger gap	d_0	9 μm
Dielectric width	d_e	0.85 μm
Initial finger overlap	l_{ol}	350 μm
Dielectric constant	ε_e	3.6
Parasitic capacitance	C_p	30 pF
Surface potential due to initial charging	V_S	200 V
Proof mass	m	2.5 g
Damping coefficient	c_d	0.9 mN·s/m
Young's modulus of main structure (silicon)	E	179 GPa

III. ANALYTICAL MODEL

The restoring force (F_r) of a curved beam can be expressed, in terms of the center displacement y_d, [19],

$$F_r = -(ky_d + k_2y_d^2 + k_3y_d^3). \quad (1)$$

k, k_2, and k_3 are linear, quadratic, and cubic spring coefficients, respectively, which can be expressed, in terms of the spring parameters as follows.

$$k = \frac{\pi^4 EWT}{12l^3}(2W^2 + 3h^2) \quad (2)$$

$$k_2 = \frac{3\pi^4 EWTh}{8l^3} \quad (3)$$

$$k_3 = \frac{\pi^4 EWT}{8l^3} \quad (4)$$

The motion equation for the device is established as follows.

$$m\ddot{y}_d + c_d\dot{y}_d = F_r + F_{elec} + F_{ext} \quad (5)$$

F_{ext} is the exerted force, i.e. ma where a is the acceleration of the environmental vibration. F_{elec} is the electrostatic force which can be expressed as, by using the voltage-source model of the electrets [18],

$$F_{elec} = \frac{1}{2}\frac{\partial}{\partial y_d}[C_1(V_S - V_1)^2 + C_2(V_S - V_2)^2]. \quad (6)$$

C_1 and C_2 are the capacitances of each of the comb-drives. V_1 and V_2 are the induced voltages in the comb-drives.

For the colored-noise analysis, (5) is modified into the following stochastic differential equations (SDE) [20].

$$dy_d = y_v dt \quad (7)$$

$$dy_v = -\frac{1}{m}[c_d y_v - F_r - F_{elec}]dt + \frac{\sigma}{m}dW_t = y_a dt \quad (8)$$

$$a = \frac{\sigma}{m}\frac{dW_t}{dt} \quad (9)$$

t is time. W_t denotes the Wiener process which models the stochastic vibration input. σ represents the diffusion coefficient that sets the input strength. y_v and y_a indicate velocity and acceleration of the mass, respectively. Euler-Maruyama method was used to solve (7-9) [21]. As the Wiener process, a random serially uncorrelated time series with standard normal distribution (i.e. white noise) was generated in MATLAB®. The random series was, then, processed through a low pass filter (cutoff: 250 Hz) to produce a colored noise signal. To this noise, the diffusion coefficient (σ) was multiplied in order to set its strength.

The accuracy of the analysis depends on the length of the input signal. Due to the capacity limit of the physical memory of the machine used for the analysis, a time series with the length of twenty million (time step: 0.1 μs) was generated as one signal. Then, the average of responses to two hundred separately generated signals was obtained for one analysis.

IV. RESULTS

In order to examine the validity of the developed model and the numerical analysis, the device was first studied with a sinusoidal acceleration (amplitude: 0.65 g; 1 g = 9.8 m/s^2), the same input condition as in the literature [17]. The obtained output power was about 1 mW, which is comparable to that reported in the literature [17].

A. Colored-Noise Acceleration

Next, the response of the energy harvesters was studied with the colored noise as the input, as described in the previous section. Fig. 2 presents an example of excitation and response signals when the input acceleration is 2 g and the

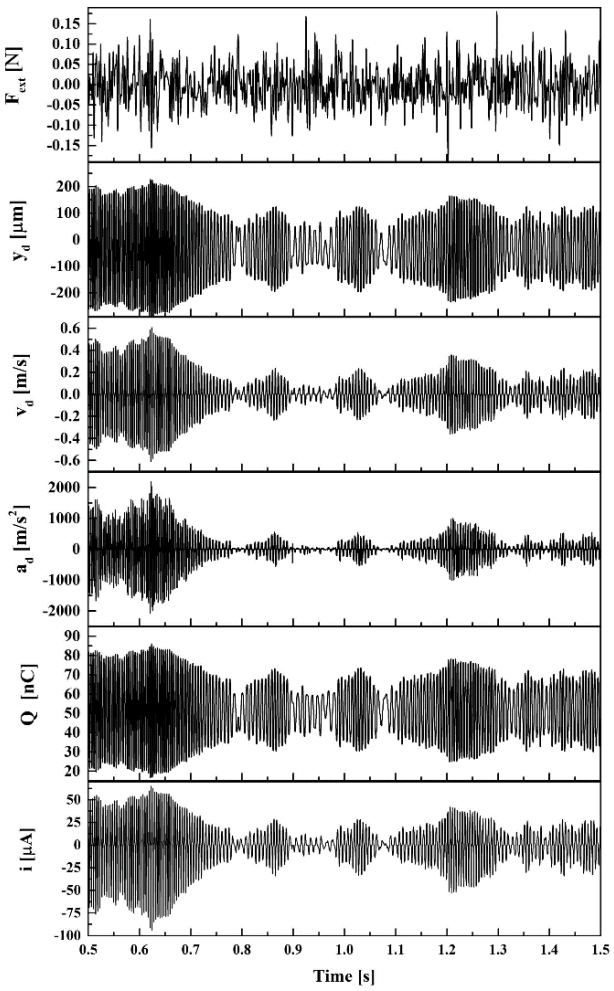

Fig. 2. An example of calculated colored-noise response; (from top to bottom) exerted force and induced responses: displacement, velocity, acceleration, charge, and current. Load resistance: 0.6 MΩ. Beam height (h): 0.5×h_{cr}. Acceleration: 2 g.

load resistance is 0.6 MΩ. The charge (Q) and the current (i) are considered only from one of the two comb-drives. The output current can be increased by summing up the currents from the two comb-drives if an adequate arrangement is made in the electric circuit. From the figure, it is evident that the magnitude of the produced current follows that of the acceleration of the structure. Fig. 3 shows examples of Poincaré maps at two different external accelerations. At lower acceleration (0.1 g), the beam stays around the original stable position. At higher acceleration (1 g), two stable positions and snapping between them can be clearly observed.

Exemplary electric power spectral densities (PSDs) are plotted in Fig. 4 for various beam heights. Beam heights are indicated as multiples of the critical beam height (h_{cr}, 69 μm for the beam width of 30 μm), which determines the bistability of the curved beam. At low beam heights, the spring nonlinearity is weak and the nonlinearity due to electrostatic force (square term) is much more prominent. A straight beam (i.e. h = 0) shows a fundamental resonant frequency of about 200 Hz. As h increases, broadening of the PSD can be clearly seen. In addition, the fundamental resonant frequency increases due to increased spring constants.

Fig. 5 presents the calculated rms powers, both electric and mechanical, for various beam heights and load resistances (R) when the input acceleration is 2 g. The following observations can be made from the results.

- The relationship between the harvested power and the beam height depends on the load resistance. For some load resistance values (e.g. 0.3 MΩ), the harvested power is maximum with the straight beam (h = 0). For other resistance values (e.g. 0.9 MΩ), there is an optimum beam height that results in the maximum electric power.
- The beam height for the best harvesting also depends on the load resistance. For example, the optimum beam height for R of 0.7 MΩ is about 1.1 h_{cr} while it is 1.5 h_{cr} for R of 0.8 MΩ. Two things happen when h increases, i.e. increase in nonlinearity as well as increase in spring constants.

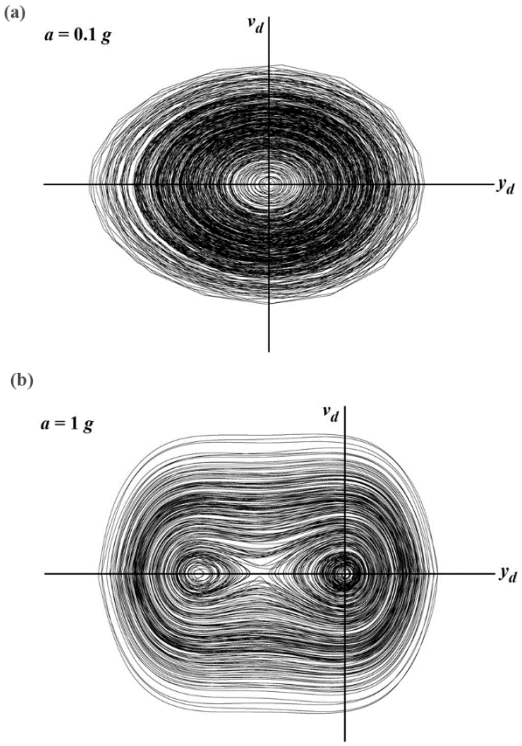

Fig. 3. Poincaré maps (velocity vs displacement). Acceleration: (a) 0.1 g and (b) 1 g. h = 1.5×h_{cr}. Two graphs are not at the same scale. The axes are with arbitrary units.

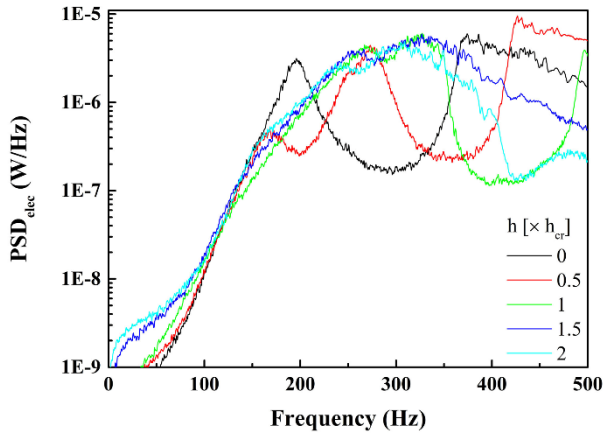

Fig. 4. Calculated electric power spectral density (PSD) for various beam heights (h). Load resistance: 0.6 MΩ. Acceleration: 2 g.

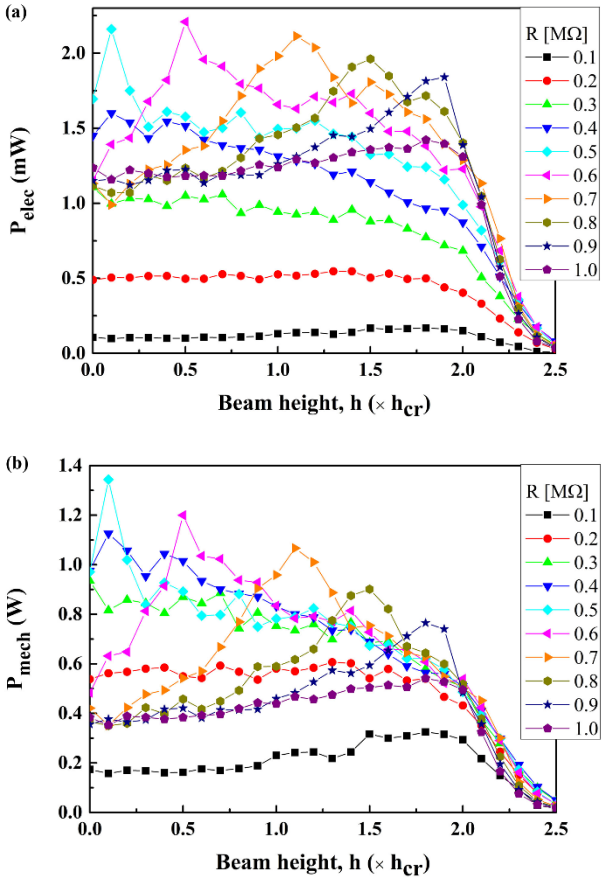

Fig. 5: Calculated (a) electric and (b) mechanical power (rms) in response to colored-noise vibration as a function of beam height for different load resistances. Acceleration: 2 g.

- The maximum mechanical power for a given load resistance is more strongly affected by the load resistance in comparison to the case of the electric power.
- Considering all the cases, the optimum load resistance is between 0.5 MΩ and 0.7 MΩ for the given input acceleration.
- Overall, the highest power is achieved as 2.69 mW when h is equal to 0.5 h_{cr} and R is 0.6 MΩ. This is about 52% higher than that of the straight beam, which shows the highest electric power of 1.77 mW when R is 0.5 MΩ.

V. Conclusion

Numerical analysis was performed to study the behavior of energy harvesting devices with electrets and balanced comb-drive configuration in response to colored-noise vibration. The effect of beam height of the curved-beam springs to the harvested energy was investigated for various loading conditions. For an input acceleration of 2 g, 52% of power improvement was observed with the optimum beam height, when compared to a straight beam spring. It should be noted that the optimum beam heights and the power improvement depend on the strength of the input acceleration. Therefore, it is necessary to examine the device performances for a specific condition of a particular application.

References

[1] Cottone F, Vocca H, and Gammaitoni L, "Nonlinear energy harvesting" Phys. Rev. Lett., vol. 102, 080601, 2009.

[2] Ferrari M, Bau M, Guizzetti M, and Ferrari V, "A single-magnet nonlinear piezoelectric converter for enhanced energy harvesting from random vibrations," Sens. Actuators A: Phys., vol. 172, pp. 287-292, 2011.

[3] Pereira TL, de Paula AS, Fabro AT, and Savi MA, "Random effects in a nonlinear vibration-based piezoelectric energy harvesting system," Int. J. Bifurcation and Chaos, vol. 29, 1950046, 2019.

[4] Xue H, Hu Y, and Wang QM, "Broadband piezoelectric energy harvesting devices using multiple bimorphs with different operating frequencies," IEEE Trans. Ultrasonics, Ferroelectrics, and Frequency Control, vol. 55, pp. 2104-2108, 2008.

[5] Xiao Z, Yang TQ, Dong Y, and Wang XC, "Energy harvester array using piezoelectric circular diaphragm for broadband vibration," Appl. Phys. Lett., vol. 104, 223904, 2014.

[6] Kim IH, Jung HJ, Lee BM, and Jang SJ, "Broadband energy-harvesting using a two degree-of-freedom vibrating body," Appl. Phys. Lett., vol. 98, 214102, 2011.

[7] Upadrashta D and Yang Y, "Trident-shaped multimodal piezoelectric energy harvester," J. Aerospace Eng., vol. 31, 04018070, 2018.

[8] Li X, Yu K, Upadrashta D, and Yang Y, "Multi-branch sandwich piezoelectric energy harvester: Mathematical modeling and validation," Smart Mater. Struct., vol. 28, 035010, 2019.

[9] Van Blarigan L, Danzl P, and Moehlis J, "A broadband vibrational energy harvester," Appl. Phys. Lett., vol. 100, 253904, 2012.

[10] Liu W, Formosa F, Badel A, Agbossou A, and Hu G, "Investigation of a buckled beam generator with elastic clamp boundary," Smart Mater. Struct., vol. 25, 115045, 2016.

[11] Eltanany AM, Yoshimura T, Fujimura N, Ebied MR, and Ali MG, "Development of piezoelectric bistable energy harvester based on buckled beam with axially constrained end condition for human motion," Japanese J. Appl. Phys., vol. 56, 10PD02, 2017.

[12] Nguyen SD and Halvorsen E, "Nonlinear springs for bandwidth-tolerant vibration energy harvesting," J. Microelectromech. Syst., vol. 20, pp. 1225-1227, 2011.

[13] Scerri J, Grech I, Gatt E, and Casha O, "Reduced-order model for MEMS PZT vibrational energy harvester exhibiting buckling bistability," Electron. Lett., vol. 51, pp. 409-411, 2015.

[14] Du H, Chau FS, and Zhou G, "Harmonically-driven snapping of a micromachined bistable mechanism with ultra-small actuation stroke," J. Microelectromech. Syst., vol. 27, pp. 34-39, 2018.

[15] Sterken T, Baert K, Puers R, Borghs G, and Mertens, R, "A new power MEMS component with variable capacitance," Mircoelectronics Symposium and Exhibition, pp. 27–34, 2003.

[16] Honma H, Mitsuya H, Hashiguchi G, Fujita H, and Toshiyoshi H, "Improvement of energy conversion effectiveness and maximum output power of electrostatic induction-type MEMS energy harvesters by using symmetric comb-electrode structures," J. Micromech. Microeng., vol. 28, 064005, 2018.

[17] Honma H, Tohyama Y, and Toshiyoshi H, "A 1.3 milliwatts electrostatic vibrational energy harvester with minimal reactive power through reduced internal stray capacitances," Transducers 2019, pp. 362-365, 2019.

[18] Yang Z, Tang L, Yu L, Tao K, and Aw K, "Modelling and analysis of an out-of-plane electret-based vibration energy harvester with AC and DC circuits," Mech. Syst. Signal Proc., vol. 140, 106660, 2020.

[19] Casals-Terre J, Fargas-Marques A, and Shkel AM, "Snap-action bistable micromechanisms actuated by nonlinear resonance," J. Microelectromech. Syst., vol. 17, pp. 1082-1093, 2008.

[20] Ando B, Baglio S, L'Episcopo G, and Trigona C, "Investigation on mechanically bistable MEMS devices for energy harvesting from vibrations," J. Microelectromech. Syst., vol. 21, pp. 779-790, 2012.

[21] Kloeden P and Platen E, Numerical solution of stochastic differential equations. New York: Springer-Verlag, 1995.